J. Marine Sci. Appl. (2012) 11: 34-43
DOI: 10.1007/s11804-012-1103-8

Experimental Evaluation of the Post-ultimate Strength Behavior of a Ship's Hull Girder in Waves

Weijun Xu, Kazuhiro Iijima*, Ryota Wada and Masahiko Fujikubo

Department of Naval Architecture and Ocean Engineering, Osaka University, Osaka 565-0871, Japan

Abstract: Experimental investigations into the collapse behavior of a box-shape hull girder subjected to extreme wave-induced loads are presented. The experiment was performed using a scaled model in a tank. In the middle of the scaled model, sacrificial specimens with circular pillar and trough shapes which respectively show different bending moment-displacement characteristics were mounted to compare the dynamic collapse characteristics of the hull girder in waves. The specimens were designed by using finite element (FE)-analysis. Prior to the tank tests, static four-point-bending tests were conducted to detect the load-carrying capacity of the hull girder. It was shown that the load-carrying capacity of a ship including reduction of the capacity after the ultimate strength can be reproduced experimentally by employing the trough type specimens. Tank tests using these specimens were performed under a focused wave in which the hull girder collapses under once and repetitive focused waves. It was shown from the multiple collapse tests that the increase rate of collapse becomes higher once the load-carrying capacity enters the reduction path while the increase rate is lower before reaching the ultimate strength.
Keywords: post-ultimate strength; collapse behavior; experimental evaluation; load-carrying capacity; hull girder
Article ID: 1671-9433(2012)01-0034-10

1 Introduction

The evaluation of post-ultimate strength is a very important issue from the viewpoint of risk-based design of hull girders. It is associated with the consequence or the risk of the hull girder, including the loss of the ship, its cargo, and human lives.

There have been many ship accidents related to structural failure. For instance, the Russian-registered tanker Nakhodka was broken up by waves after heavy corrosion of plates and caused a large oil spill, polluting the Sea of Japan coast. The M/V Erika and Prestige were broken up, and a vast amount of oil was spilled into the coast of France (December 1999) and Spain (November 2002), respectively. The importance of accidents is dependent on the amount of loss. Assuming that the amount of loss is closely related to the severity of the collapse, more attention should be paid to the behavior of post-ultimate strength. Specifically, to what extent the structure may collapse should be addressed.

Many researchers have tried to clarify the post-ultimate strength behavior from a structural engineer's viewpoint. To name a few, Smith (1977) was the first to obtain the bending moment-curvature relationship including the ultimate strength and post-ultimate strength. Rutherford and Caldwell (1990) proposed an analytical method to predict the post-ultimate strength behavior using the ultimate strength formulae and solution of the rigid-plastic mechanism analysis. Chen *et al.* (1983) presented a general finite element approach for the collapse analysis of a ship's hull. An alternative method for performing progressive collapse analysis is the Idealized Structural Unit Method (ISUM), which was originally proposed by Ueda and Rashed (1984) to perform progressive collapse analysis on the transverse frame of a ship structure. ISUM rectangular plate and stiffened panel elements were developed by Ueda *et al.* based on the effective width concept, and they were implemented in ALPS/ISUM by Paik *et al*. (1996). A new concept of ISUM plate element introducing the shape functions for deflection was proposed by Masaoka *et al*. (1998) and it was further extended to an ISUM stiffened panel model by Fujikubo and Kaeding (2002). This newest version of ISUM stiffened panel models was successfully applied to the progressive collapse analysis of hull girder cross sections by Pei and Fujikubo (2005).

Yao and Nikolov (1991, 1992) proposed a simple and practical analytical method to simulate progressive collapse behavior of a ship's hull subjected to longitudinal bending based on Smith's method, so as to estimate the load-carrying capacity of a ship's hull including post-ultimate strength behavior. In their method, progressive loss in rigidity due to the occurrence of local buckling and yielding were taken into account. Both flexural bucking and flexural-torsional buckling were considered for the deflection mode of a stiffener. Recent developments may be found in Yao *et al*. (2006).

Experimental investigations have also been made. Sugimura *et al*. (1966) carried out a collapse test on a 1/5-scale welded steel hull girder model of a destroyer escort ship. Reckling

Received date: 2011-11-14.
Foundation item: Supported by the Ministry of Education, Science, Sports, and Culture, Grant-in-aid for Scientific Research (A), (23246150), 2011.
***Corresponding author Email:** Iijima@naoe.eng.osaka-u.ac.jp

(1979) performed a series of collapse tests on seven box-girder models under pure bending, and Ostapenko (1981) performed tests on three box-girder models applying combined bending, shear, and torsional loads. Nishihara (1983) tested eight box-girder models representing a single hull tanker, a double-hull tanker, a bulk carrier, and a container ship. Dow (1991) also carried out a collapse test on a 1/3-scale welded steel hull girder model of a Leander class frigate. In Sugimura and Dow's tests, the sagging bending moment was applied on the model, and the buckling of the deck and the upper part of the side shell plating led to the overall collapse of a cross-section. Endo *et al*. (1988) and Yao *et al*. (2002) conducted a series of collapse tests on hull girder models. For Endo's tests, the shearing force and bending moment were applied simultaneously simulating a slamming load, and the occurrence of buckling at the deck and yielding of the side shell plating was the trigger for the overall collapse of a cross-section. For Yao's tests, the cross-section collapsed very quickly after the occurrence of overall buckling of the deck as a stiffened plate and local buckling of the upper side shell plating. Collapse tests on stiffened box girder models have also been carried out. Mansour (1995) carried out similar tests on two models applying distributed lateral loads by air pressure through air-bags. One is to simulate collapse behavior of a single-hull tanker, and the other to simulate different collapse behaviors. Gordo and Guedes Soares (2004, 2007) tested box girders subjected to a pure bending moment until collapse. The moment curvature curves were presented allowing for the analysis of elastic-plastic behavior until collapse and the evaluation of the ultimate bending moment as well as the post collapse behavior.

However, as far as the present authors know, these analyses and tests could not be utilized to give an answer to the former question, namely to what extent the ship structure may collapse. To answer this question, interaction between fluid and structure needs to be considered since the inertia force, hydrostatic forces and hydrodynamic force play a significant role in the dynamic collapse behavior as pointed out by Yao *et al*. (2009). For tank tests, a scaled model to reproduce the dynamic collapse behavior is necessary and has been developed by Wada *at el.* (2010). Correspondingly, a hydroelasto-plasticity approach was proposed by Kimura *at el*. (2010) and Xu *at el*. (2011). Iijima *at el*. (2011) detailed this approach and clarified the post-ultimate strength behavior characteristics in waves by using the numerical and tank test results. The post-ultimate strength behavior of a ship's hull girder in waves was investigated by Xu *at el.* (2011) by using analytical solutions.

The present investigations primarily focus on evaluating experimentally the post-ultimate strength behavior of a hull girder by using a scaled box-shape ship in waves. The whole ship is modeled by two rigid bodies connected to each other amidship by a special device. The device includes sacrificial specimens. Various load carrying capacities of the hull girder may be reproduced by changing the specimens. Static and dynamic collapse test results of the scaled model, on which different types of specimens are mounted, are reported.

2 Model design methodology

2.1 General introduction of model

To investigate the post-ultimate strength behavior of a box-shape generic ship hull girder in waves, a ship was modeled by two rigid bodies connected to each other amidship by a device. The device includes a hinge at deck level, while a sacrificial beam specimen is fixed to the bottom of the ship's fore body and connected to the ship's aft body by a rigid boom. The scale ratio of the model is assumed to be 1/100. Based on a generic ship which has a length of 300 m, breadth of 40 m, depth of 30 m, and draft of 10 m, the main particulars of the model are 3 m length, 0.4 m breadth, 0.3 m depth, and 0.1 m draught. The sketch of the experimental model for fabrication is shown in Fig.1.

The model includes four parts:

1) Model A (body 1): the right body in Fig.1. Made of wood, 1 462 mm in length, 300 mm in height, and 400 mm in width.

2) Model B (body 2): the left body in Fig.1, the same dimensions as model A.

3) Middle part: a device consisting of two blocks of aluminum plates, each attached to Model A and Model B. At the top of the aluminum plate on Model A, the plate is connected to another aluminum plate (lever plate) by a hinge around which the model can rotate. A potentiometer is set up there to detect the rotational angle. The lever's height is 400mm. At the bottom of the lever plate, a boom is extended horizontally to be connected to a sacrificial specimen. The other end of the specimen is fixed to a rigid aluminum block located below Model A. Therefore, the shear force can be borne by the specimen. Three load cells are installed between the lever plate and the aluminum plate on Model B. Pure hull girder bending moments can be detected after excluding the effect of axial forces by using the measurement on the load cells.

4) Backbone: a steel pipe with a rectangular cross section. It is only for preventing a large bending moment on the hull girder during installation work. The backbone is removed when conducting collapse tests.

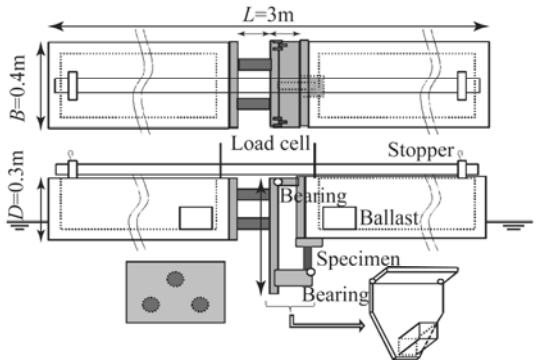

Fig.1 Sketch of the experimental model for fabrication

2.2 Model requirements and design idea

The scaled model needs to follow the law of similitude in terms of strength as well as geometry and stiffness. The design methodology is detailed in Wada *et al*. (2010).

The requirements for the scaled model are, a) to realize the strength model of the hull girder collapse behavior in loading and unloading as shown in Fig.2; b) to collapse in waves which can be generated in the tank; c) to be free from severe wave-induced vibrations; d) to be available for repeated collapse tests. Concerning a), the reduction of strength in the post-ultimate strength range, shown as Fig.2, is typical in the hull girder collapse accompanied by buckling of stiffened panels, and thus to be considered.

The requirement b) is interpreted as keeping the law of similitude in 'strength' itself. The scaled model must collapse under wave loads which are scaled according to Froude's law. The hull girder strength of the model must be low enough in this regard. The design value of the wave bending moment M_w may be roughly given for the design work in terms of non-dimensional value as follows:

$$\frac{M_w}{\rho g L^2 B \eta} = 0.02 \tag{1}$$

where, L and B are the length and breadth of the model hull, ρ is the density of water, g is the gravity acceleration, and η is the wave amplitude. For the tank tests, the maximum wave amplitude may be taken as η = 100 mm.

The requirement c) necessitates keeping the law of similitude in stiffness as well. The model must be also rigid enough so that the natural frequency is out of the wave frequency range which is normally from 0.5 to 2 Hz in the model scale. The two requirements b) and c) may contradict each other.

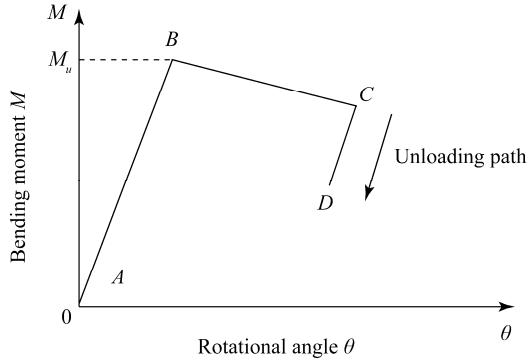

Fig.2 Strength model

The scaled model design in Fig.1 meets the above requirements. The scaled model has a weight of 55.2 kg, the gravity height based on the bottom of the model is 113 mm, the radius of gyration is 264 mm, and the inertia moment of the respective part of the hull model is 17.4 kg·m^2. The nonlinear relationship between the moments and rotational angle may be represented by the collapse mechanism of the specimen. The yielding point should occur at the upper end of the specimen, as the bending moment is the largest there.

2.3 Specimens

A selection of a specimen which shows an appropriate bending moment-rotational displacement relationship is a key to the scaled model. In this research, a circular pillar specimen with a 10 mm diameter cut out from a block of SS400 steel was first adopted. This specimen is termed No.0. However, as mentioned later, the specimen could not reproduce the reduction of the load-carrying capacity after the ultimate strength as shown in Fig.2, and other types of specimens were invented. In the new specimens, the cross section of the beam near the fixed end has a U-shape with two small slits (See Fig.3). It is anticipated that the plate may buckle and yield under bending moments and show the reduction after the ultimate strength. These specimens are termed trough type specimens.

Table 1 Principle specifications of the specimens

Parameters	No.1	No.2	No.3
H/mm	40	40	40
h/mm	10	11	11
b/mm	12	12	12
t_1/mm	2	2	2
t_2/mm	2	4	3
h_1/mm	7	6	6
b_1/mm	6	6	6
The plastic bending moments for the whole section/(N·m)	25.97	35.28	32.52
Load-carrying capacity /(N·m)	12.005	8.82	8.82
Wave bending moment /(N·m)	101.15	137.41	126.67
Moment of inertia ($\times 10^{-10}$)/m^4	3.72	5.36	5.20
The ratio of moment of inertia to the circular pillar	0.76	1.09	1.06

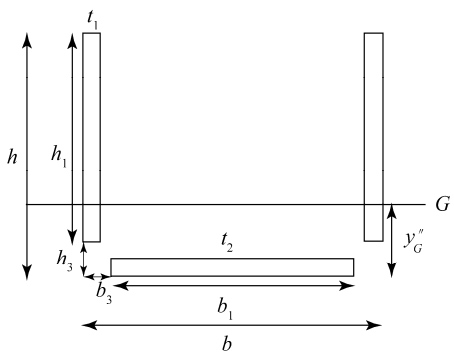

(a) Section of the trough type specimen

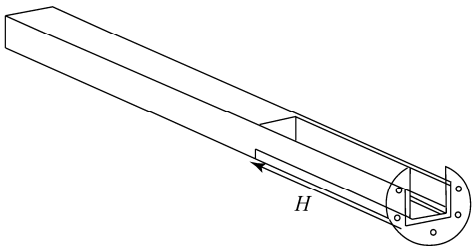

(b) Schematic diagram of the trough type specimen

Fig.3 Section and the schematic diagram of the trough type specimen

The principal specifications of the new specimens are listed in Table 1. For the trough type specimens, there are three kinds of dimensions, which are denoted as No.1, No.2, and No.3. The scantlings of the specimens were determined by using nonlinear FE calculations taking the strain hardening effects into account. The specimens were produced by machining.

3 Calculation result by FEM

In order to confirm the final scantlings of the model, a series of numerical simulations was performed before tests on the ground and in the tank. The dimensions and material properties employed for the FE model are listed in the Table 2. The whole FE model is illustrated in Fig.4.

The natural frequencies were analyzed by FE analysis software Abaqus under different ballast scenarios. The natural frequencies for the various ballast scenarios are presented in Table 3. From the calculation results in Table 3, it can be observed that the natural frequencies of the model ship in different ballast conditions are out of the wave frequency, which normally ranges from 0.5 to 2 Hz in model scale.

Table 2 Types and properties of material in the FE model

Material type	Properties	Values
	Shell element	
Wood	Young's modulus E/GPa	8.8
	Density/(kg·m^{-3})	0.41×10^3
	Beam element	
ss400	Young's modulus E/GPa	206
	Yield stress σ_y/MPa	245
	Density/(kg·m^{-3})	7.8×10^3
	Shell element	
Aluminum	Young's modulus E/GPa	70
	Density/(kg·m^{-3})	2.7×10^3

Table 3 Natural frequencies of the model ship for different ballast conditions Hz

Ballast condition	Natural frequency
Ballasts are located near the center of the model ship	7.40
Ballasts are located near the ends of the model ship	3.04
Ballasts are uniformly distributed along the inner bottom of the model ship	4.45

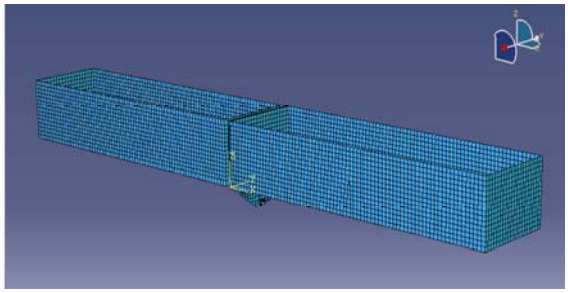

Fig.4 The whole FE model

4 Experimental results by ground test and tank test

4.1 Experimental results by ground test

Prior to the tank tests, static four-point-bending tests were conducted to detect the load-carrying capacity of the hull girder. A schematic diagram is shown in Fig.5. Around the middle part, there are two supporting points using an angle bar and a steel tube which were respectively used to restrain the horizontal movement and to allow the horizontal movement. Then, only the bending moment is exerted on the hull girder excluding the axial load. Two blocks of rubber were settled under the angle bar and steel tube to prevent them from slipping. Two belts connected with chain hoists were used to lift the model at the both ends of the model. Thus, the experiment was performed by additionally giving the forced displacement at both ends.

Fig.6 shows the results of the three ground tests when No.0 specimen was mounted. The vertical axis shows the vertical bending moment over the hull girder in sagging condition. Repeatability of the tests can also be confirmed. It is found that the collapsing moment of the hull girder is 180 N·m in the scaled model (See Fig.6). The reduction of load-carrying capacity after the ultimate strength is not realized by using the specimen No.0 since only yielding occurs in the specimen whereas the capacity reduction is accompanied by buckling. In the figure, FE-analysis results in which solid elements are employed and the material is assumed to be perfectly elastic plastic are also presented. The discrepancies may be attributed to the strain hardening effects which were not accounted for in the FE-analysis.

Fig.7 shows the ground test results for specimens Nos.1−3. It is observed that the reduction of load-carrying capacity is reproduced for specimens Nos.1 and 3 while the load-carrying capacity is almost constant for specimen No.2 after the ultimate strength. A buckling collapse for the trough type specimens is attributed to these characteristics. Numerical analysis results from using the FEM are plotted in the same figure. Although there is some difference between the FEM and the ground test results, the numerical results can explain the above characteristics which satisfy the model requirement a) mentioned in section 2.2.

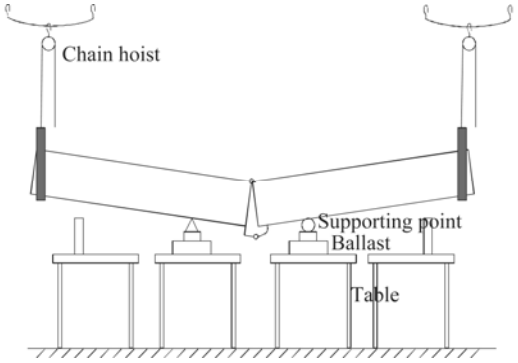

Fig.5 Schematic diagram of static four-point-bending tests

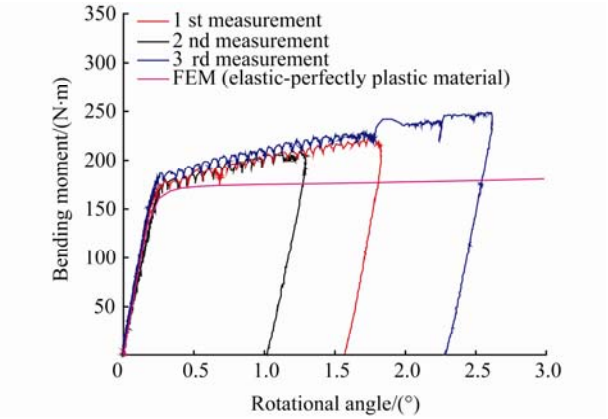

Fig.6 Moment-rotational angle relationship of the pillar type specimens measured in the ground test

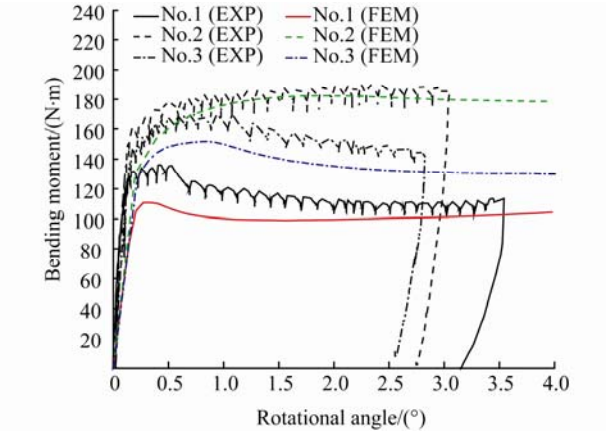

Fig.7 Comparison of the relationship between the bending moment and the rotational angle for three kinds of specimens by FEM and the experiments

(a) Before the test (b) After the test

Fig.8 Comparison of deformations; the circular pillar type specimen (No.0)

(a) After deformation of No.1 (b) After deformation of No.2

(c) After deformation of No.3 (d) Before deformation of No.3

Fig.9 Comparison of deformations; the trough type specimens Nos.1–3

Figs.8 and 9 compare the deformation shapes of the respective specimens. It can be observed that the deformation occurs at the joint part between the flange and the circular pillar No.0. Yielding may have been induced at the part. For specimens No.1 and 3, the plate shows a buckling deformation which leads to the reduction of the load-carrying capacity of the hull girder in bending. For

specimen No.2, the buckling deformation was not clearly observed as the plate is a little too thick.

4.2 Experimental results by tank test

4.2.1 Experimental setup

A series of tank tests was conducted in the towing tank at Osaka University. The tank is 100 m in length, 7.8 m in breadth, and 4.3 m in depth, and a plunger wave maker is set at the end of the towing tank which can generate the long-crested wave. For this test, the towing carriage was settled at the middle of the tank, or 50 m away from the wave maker. The towing carriage provided the operating platform for the tank test. The ship model was installed at the towing carriage. No forward speed was given. In addition to the three load cells and the potentiometer, four acceleration transducers were mounted to measure the vertical bending moment of the hull girder in the midship section, rotational angle between the two bodies, and rotational accelerations of the respective bodies. Two wave probes were also fixed in the tank, one in front of the wave maker, located 12 m position away from the wave maker, the other at the center of the tank. All this data was sampled simultaneously at a frequency of 50 Hz, and transferred to PC. The configurations of the tank test and the measurement system are shown in Fig.10 and Fig.11, respectively. The scaled model hull in the tank test and the photo zoom-up of the midship are shown in Fig.12 and Fig.13. In Fig.13, the part surrounded by broken lines shows the specimen.

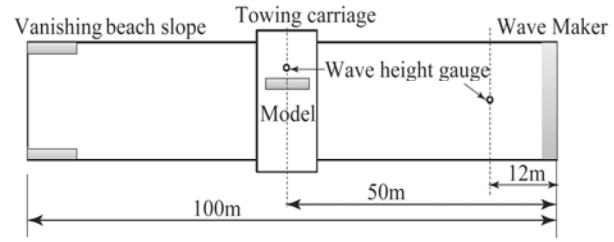

Fig.10 Tank test configurations

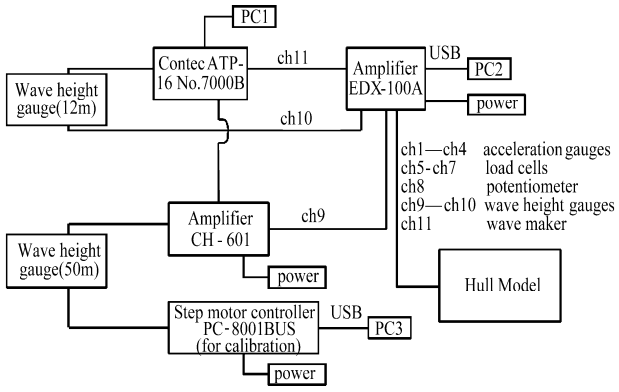

Fig.11 Diagram of measurement system

4.2.2 Towing tank test procedure

In this test, a focused wave technique using the First Order Reliability Theory (FORM) was employed to generate a large single wave (Jensen and Capul, 2006; Iijima *et al*. 2011). Calibrations of the wave maker for generating regular and irregular waves were conducted to obtain the transfer functions between the input voltage to the wave maker and the wave elevation at the center of the tank. A target-focused wave was generated from the International Ship and Offshore Structures Congress (ISSC) wave spectrum with a significant wave height of H_S=20.0 cm (20.0 m) and with a mean wave period of T_0=1.39 s (13.9 s). The values in the parenthesis show the values in real scale. The focused wave was intended to occur with its trough around the midship part of the model at around t=80 s so that it would induce maximum sagging moment amidship.

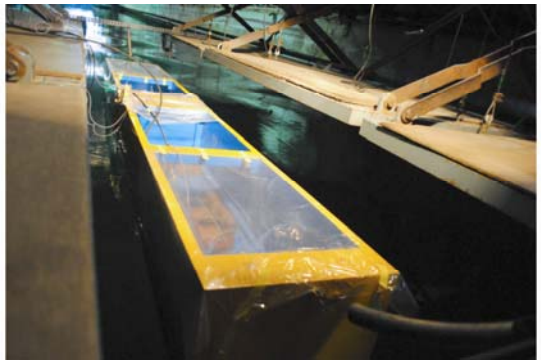

Fig.12 Scaled model hull in tank test

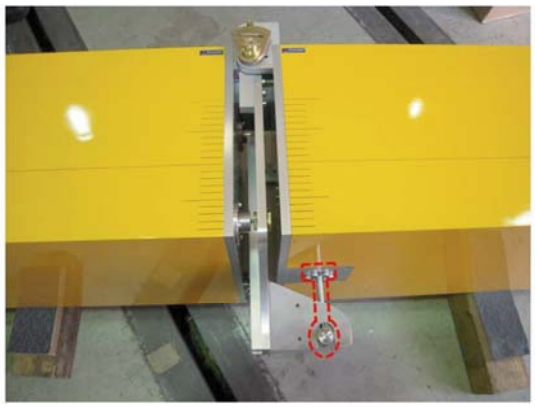

Fig.13 Photo zoom-up of the midship (the part surrounded by broken lines shows the specimen)

Ballasts were loaded so that the target draft and target still-water bending moment in sagging were attained simultaneously. The total ballasts amounted to 588 N. The still-water bending moment in sagging was measured to be 90 N·m in scaled model tests using the specimen No.0 while it was 110 N·m for the tests using the specimens Nos.1−3.

As a preliminary check, the natural frequency of the model was measured by a hammering test. For the specimen No.0 and No.1, when all the ballasts were loaded, the natural frequency was found to be around 7 Hz (44 rad/s) for scaled model, or 0.7 Hz (4.4 rad/s) in a real scale ship. The natural frequencies were confirmed to be out of the wave frequency range from 0.2 rad/s to 1.5 rad/s in real scale. The critical damping ratio γ was also detected to be 1.8%.

Finally, a series of collapse tests was conducted under the focused wave. A sample time history of the focused wave measured in the tank test is shown in Fig.14. The maximum wave trough in this wave train is approximately 0.18 (m) in model scale. When the negative trough peak reaches the midship part, the wave-induced bending moment acts on the midship of the model in sagging condition, and the hull girder collapses when a sum of the still-water and wave-induced bending moments exceeds the ultimate strength.

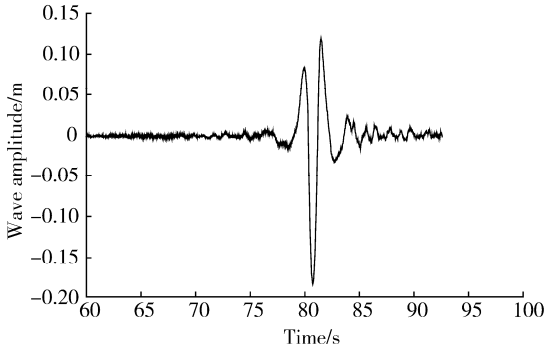

Fig.14 Time history of wave elevation measured in the tank test

4.2.3 Collapse Test in Tank

1) The circular pillar type specimen

A series of tank tests using the circular pillar type specimen was repeated 5 times. The hull girder was intended to collapse once under a single large wave, also known as the focused wave. In each test, the sacrificial specimen was replaced. The experimental case tests are denoted as Nos.4001−4005, respectively. The time histories of the rotational angle of the hull girder for all specimens and the relationships between the vertical bending moment of the hull girder and the rotational angle are plotted in Figs.15 and 16, respectively. As these tests were performed under almost the same focused wave, however, its amplitude has slight scatter as the position of the carriage was moved back and forth to obtain the largest wave through the amidship; the test results do not show the same results. The case No.4005 experienced the largest amplitude of the focused wave.

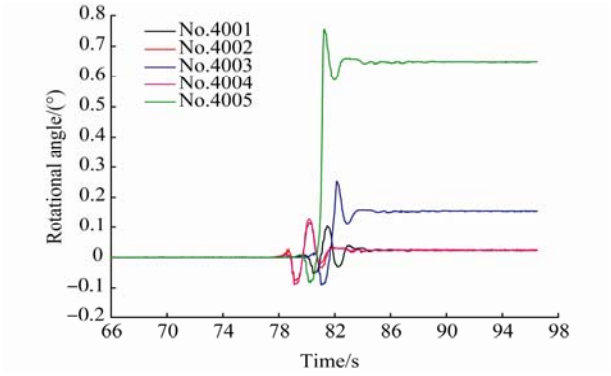

Fig.15 Time history of rotational angle for No.4001–No.4005 specimens

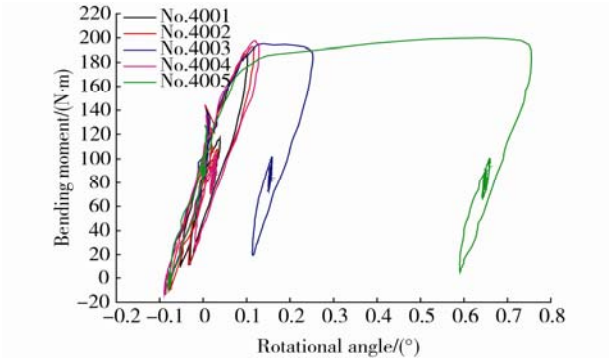

Fig.16 Relationship between the bending moment and the rotational angle for No.4001–No.4005 specimens

From the results of No.4005 in the Figs.15 and 16, it can be observed that when the time instance reaches around t=80s, the rotational angle begins to decrease by about 0.08 degrees, then increase rapidly around to around 0.76º at t=81 s. After a little fall back, it maintains an almost constant quantity around 0.65º. Hence, it can be seen that about 0.65º of plastic deformation was formed due to the extreme wave-induced bending moment.

It is clearly observed that the measurement results for the circular pillar type specimen in the Fig.16 show the increase of the load-carrying capacity after the collapsing moments, which is consistent with the ground test results.

2) The trough type specimens

A series of tank tests for the specimens Nos.1–3 was conducted under a similar focused wave. However, the amplitude of the focused wave could not be increased as much as that for specimen No.0, since the limiter control for the wave maker had been renewed and a smaller value had been given to it. In addition to a single collapse, a multiple collapse, in which a focused wave was applied repeatedly for a model with the same specimen, was investigated to clarify the collapse behavior in irregular seas with multiple extreme waves.

The dynamic collapse tests for specimen No.1 were conducted 10 times in total. The tests are denoted as collapse 0082−0091, respectively. The relationships between the vertical bending moment and rotational angle measured during the tests from collapse 0082 to collapse 0088 are plotted in Fig.17. The whole collapse test results are plotted in the same manner as shown in Fig.18. As for collapse 0089 and collapse 0090, the whole time history was not obtained because the signal from the potentiometer went out of the measurable range. Also, the signals before it left the range and the last part signals of the collapse could be captured. The signals which could not be captured were reconstructed by connecting these measured signals using a smooth line in the figure.

From Fig.17, it can be found that from collapse 0082 to collapse 0088, the cycles are moving towards the right hand

side. This indicates that the plastic deformation is progressing with the spread of yielding. For the first cycle (collapse 0082), comparatively large plastic deformation was formed, while from the second cycle (collapse 0083) to the fifth cycle (collapse 0086), there was almost no additional plastic deformation formed. That is because the load-carrying capacity increases even after reaching the collapsing moment in the first cycle while the extreme loads are constant.

Slightly larger amplitude of the focused wave was applied for collapse 0087 and collapse 0088 and even larger extreme loads were exerted on the hull girder. Then, the increase rate of plastic deformation increased following the path with reduction of load-carrying capacity. To sum it up, the increase rate of plastic deformation was slow at the beginning of the collapse but gained when the collapse started to enter the path with the reduction of load carrying capacity.

From Fig.18, it can be found that the ground test result is plotted in black dashed line for the No.1 specimen. The tank test and the ground test have almost the same ultimate strength and collapse behavior; they show the reduction tendency after reaching the ultimate strength and tend to be gentle with the increase of the rotational angle. This indicates that the load-carrying capacity of the hull girder in the middle-section is a kind of intrinsic property due to its material and structure, irrespective of the external load exerted.

For the collapse tests with the No.2 specimen, nearly the same focused wave was repeated three times, and consequently the hull girder collapsed three times. The tests are denoted as collapse 0076, collapse 0077, and collapse 0080, respectively. The time histories of the rotational angle of the hull girder for the respective collapse tests are given in Fig.19. The corresponding relationships between the vertical bending moment amidship and the rotational angle are also plotted as shown in Fig.20.

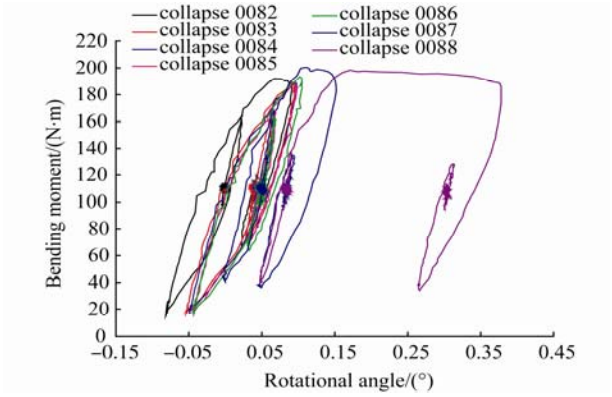

Fig.17 Relationship between bending moment and rotational angle for progressive collapse test of the No.1 specimen from collapse 0082 to collapse 0088

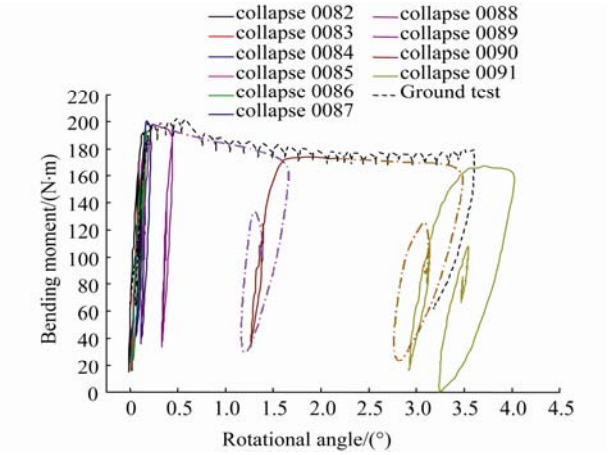

Fig.18 Relationship between bending moment and rotational angle for complete progressive collapse loading and unloading cycle tests

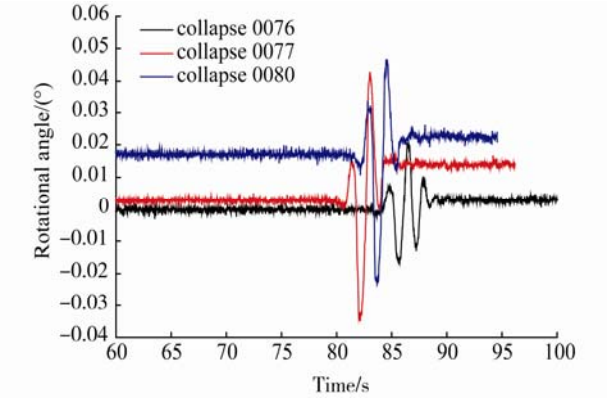

Fig.19 Time history of the rotational angle for the collapse test of the No.2 specimen

The dynamic collapse tests for specimen No.3 were conducted twice, denoted as collapse 0096 and collapse 0097. The time histories of the rotational angle of the specimen are plotted in Fig.21. Also, the relationships between the bending moment and the rotational angle are given in Fig.22. The progress of the plastic deformation is slow.

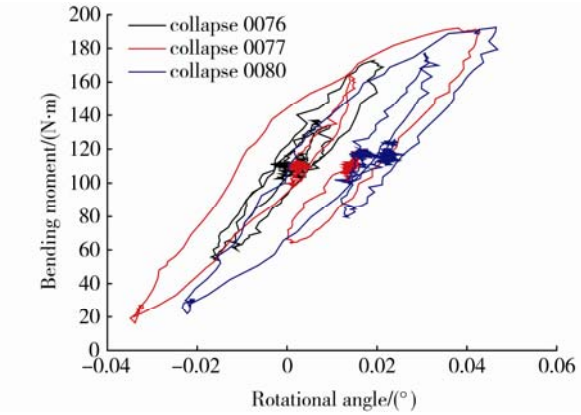

Fig.20 Relationship between the bending moment and the rotational angle for the collapse test of the No.2 specimen

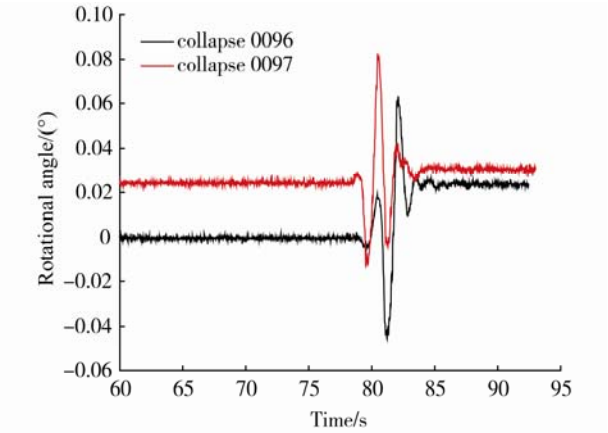

Fig.21 Time history of the rotational angle for the collapse test of the No.3 specimen

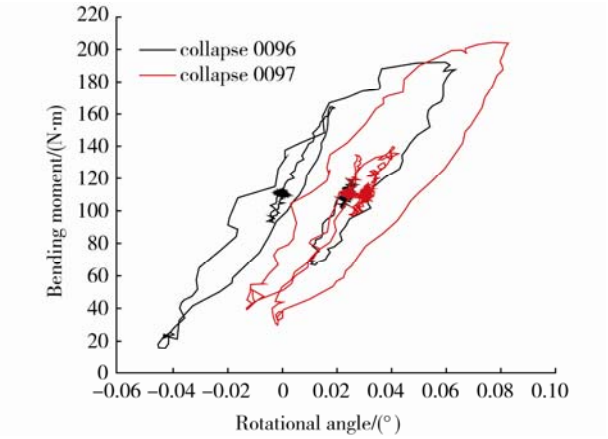

Fig.22 Relationship between bending moment and rotational angle for progressive collapse test of the No.3 specimen from collapse 0096 to collapse 0097

Table 4 Summary of the severities for the trough specimen in tank tests

Specimen Nos.	Collapse cases	Severity /(°)	Remarks
No.1	Collapse 0082	0.107	Initial case for No.1
	Collapse 0083	0.006	
	Collapse 0084	0.004	
	Collapse 0085	0.0004	
	Collapse 0086	0.0005	
	Collapse 0087	0.033	Wave amplitude increased hereafter
	Collapse 0088	0.221	
	Collapse 0089	1.008	
	Collapse 0090	1.731	
	Collapse 0091	0.369	
No.2	Collapse 0076	0.003	Initial case for No.2
	Collapse 0077	0.014	
	Collapse 0080	0.006	
No.3	Collapse 0096	0.024	Initial case for No.3
	Collapse 0097	0.007	

For the trough type specimens, the severities of each collapse case in the tank tests are summarized in Table 4. It can be observed that the severity of the first collapse under a single large wave is 0.107º, 0.003º, and 0.024º, respectively, for specimens No.1, No.2, and No.3. The order can be explained by the order of magnitude of ultimate strength. i.e., the hull girder capacity is the largest for the specimen No.2, then No.3, and No.1, in that order.

5 Conclusive remarks

The collapse behavior of a hull girder subjected to extreme wave-induced loads was investigated experimentally. The scaled model design was developed, and a series of ground and tank tests were reported. The conclusions are summarized as follows.

1) The trough type specimens can reproduce the bending moment-rotational displacement relationship including the reduction of load-carrying capacity after reaching ultimate strength. These properties are considered to accurately represent those of an actual ship.

2) The severity of collapse in a large single wave is the largest for the trough type specimen No.1, then No.3, and No.2, in that order. The order is determined mostly by the ultimate strength of the specimens, i.e., the smaller severity for the specimen with the larger ultimate strength.

3) As for a multiple collapse, the increase rate of severity is small at the beginning of the cycles. However, it increases once it starts to enter the path having reduction of load-carrying capacity.

Acknowledgement

Mr. Goto, Y., Ms. Suzaki, Y., Mr. Goto, M., and Mr. Kimura, K. are acknowledged for their support in conducting the tests.

References

Chen KY, Kutt LM, Piaszczyk CM, Bieniek MP (1983). Ultimate strength of ship structures. *SNAME Transactions*, **91**, 149-68.

Dow RS (1991). Testing and analysis of 1/3-scale welded steel frigate model. *Proceedings of the International Conference on Advances in Marine Structures*, Dunfermline, Scotland, 749-773.

Endo H, Tanaka Y, Aoki G, Inoue H, Yamamoto Y (1988). Longitudinal strength of the fore body of ships suffering from slamming. *J Soc Naval Arch Japan*, **163**, 322-333. (in Japanese)

Fujikubo M, Kaeding P (2002). New simplified approach to collapse analysis of stiffened plates. *Marine Structures,* **15**(3), 251-283.

Gordo JM, Guedes Soares C (2004). Experimental evaluation of the ultimate bending moment of a box girder. *Marine Systems and Ocean Technology*, **1**(1), 33-46.

Gordo JM, Guedes Soares C (2007). Experimental evaluation of the behaviour of a mild steel box girder under bending moment. *Advancements in Marine Structures*, Guedes Soares C and Das PK (Eds.), Taylor & Francis Group, London, UK, 377-383.

Iijima K, Kimura K, Xu W, Fujikubo M (2011). Hydroelasto-plasticity approach to predicting the post-ultimate strength behavior of ship's hull girder in waves. *Journal of Marine Science and Technology*, **16**(4), 379-389.

Jensen JJ, Capul J (2006). Extreme response predictions for jack-up units in second order stochastic wave by FORM. *Probabilistic Engineering Mechanics*, **21**(4), 330-337.

Kimura K, Iijima K, Wada R, Xu W, Fujikubo M (2010). Dynamic collapse behavior of ship's hull girder in waves. *Advanced Maritime Engineering Conference and 4th Pan Asian Association of Maritime Engineering Societies Forum*, Singapore, 261-266.

Mansour AE, Lin YH, Paik JK (1995). Ultimate strength of ships under combined vertical and horizontal moments. *Proceedings of the Sixth International Symposium on PRADS*, Seoul, Korea, 844-851.

Masaoka K, Okada H, Ueda, Y (1998). A rectangular plate element for ultimate strength analysis. *Second International Conference on Thin-Walled Structures*, Singapore, 469-476.

Nishihara S (1983). Analysis of ultimate strength of stiffened rectangular plate (4th Report)—on the ultimate bending moment of ship hull girder. *J Soc Naval Arch Japan*, **154**, 367-375. (in Japanese)

Ostapenko A (1981). Strength of ship hull girders under moment, shear and torque. *Proceedings of the SSCSNAME Symposium on Extreme Loads Response*, Arlington, USA, 149-166.

Paik JK, Thayamballi AK, Che JS (1996). Ultimate strength of ship hulls under combined vertical bending, horizontal bending and shearing forces. *SNAME Transactions*, **104**, 31-59.

Pei ZY, Fujikubo M (2005). Application of Idealized Structural Unit Method to progressive collapse analysis of ship's hull girder under longitudinal bending. *Proceedings of the Fifteenth International Offshore and Polar Engineering Conference, ISOPE2005*, Seoul, Korea, 766-773.

Reckling KA (1979). Behaviour of box girders under bending and shear. *Proceedings of the ISSC*, Paris, France, 46-49.

Rutherford SE, Cardwell JB (1990). Ultimate longitudinal bending strength of ships: A case study. *SNAME Transactions*, **98**, 441-471.

Smith CS (1977). Influence of local compressive failure on ultimate longitudinal strength of a ship's hull. *Proc. Proceedings of the International Symposium on Practical Design in Shipbuilding*, Tokyo, Japan, 73-79.

Sugimura T, Nozaki M, Suzuki T (1966). Destructive experiment of ship hull model under longitudinal bending. *J Soc Naval Arch Japan*, **119**, 209-220. (in Japanese)

Ueda Y, Rashed SMH (1984). The idealized structural unit method and its application to deep girder structures. *Computers and Structures*, **18**(2), 227-293.

Ueda Y, Rashed SMH, Paik JK (1984). Plate and stiffened plate units of the idealized structural unit method (1st Report). *J Soc Naval Arch Japan,* **156**, 366-377. (in Japanese)

Wada R, Iijima K, Kimura K, Xu W, Fujikubo M (2010). Development of a design methodology for a scaled model for hydro-elastoplasticity of a hull girder in waves. *Advanced Maritime Engineering Conference and 4th Pan Asian Association of Maritime Engineering Societies Forum*, Singapore, 248-253.

Xu W, Iijima K, Fujikubo M (2011). Hydro-elastoplasticity approach to ship's hull girder collapse behavior in waves. *Advancements in Marine Structures*, Guedes Soares C and Fricke W (Eds.), Taylor & Francis Group, Hamburg, Germany, 239-247.

Xu W, Iijima K, Fujikubo M (2011). Investigation into post-ultimate strength behavior of ship's hull girder in waves by analytical solution. *Proceedings of the 30th International Conference on Ocean, Offshore and Arctic Engineering, OMAE2011*, Rotterdam, Netherland, OMAE2011-49617.

Yao T, Brunner E, Cho SR, Choo YS, Czujko J, Estefen SF, Gordo JM, Hess PE, Naar H, Pu Y, Rigo P, Wan ZQ (2006). Report of Committee III.1: Ultimate Strength. *Proc. 16th ISSC*, Southampton, UK, 359-443.

Yao T, Fujikubo M, Iijima K, Pei Z (2009). Total system including capacity calculation applying ISUM/FEM and loads calculation for progressive collapse analysis of ship's hull girder in longitudinal bending. *Proceedings of the 19th International Offshore and Polar Engineering Conference, ISOPE2009*, Osaka, Japan, 706-713.

Yao T, Fujikubo M. Yanagihara D, Fujii I, Matrui R, Furui N, Kuwamura Y (2002). Buckling collapse strength of chip carrier under longitudinal bending (1st Report)—collapse test on 1/10-scale hull girder model under pure bending. *J Soc Naval Arch Japan*, **191**, 265-274 (in Japanese).

Yao T, Nikolov PI (1991). Progressive collapse analysis of a ship's hull under longitudinal bending. *J Soc Naval Arch Japan*, **170**, 449-461.

Yao T, Nikolov PI (1992). Progressive collapse analysis of a ship's hull under longitudinal bending (2nd Report). *J Soc Naval Arch of Japan*, **172**, 437-446.

Weijun Xu was born in 1973. He is an associate professor at Harbin Engineering University. He is currently working towards his PhD degree in Naval Architecture and Ocean Engineering at Osaka University, Japan. His current research interests include post-ultimate strength behavior of ships, offshore structures, and the Hydroelasto-plasticity approach.

Kazuhiro Iijima was born in 1971. He is an associate professor at Osaka University, Japan. His current research interests include springing and whipping of ocean-going vessels, risk assessment of ships, and response analysis of offshore structures under wind and wave loads.

Ryota Wada was born in 1987. He is currently working towards his master's degree in Naval Architecture and Ocean Engineering at Osaka University, Japan. His current research interests include model design and post-ultimate strength behavior of ships and offshore structures.

Masahiko Fujikubo was born in 1957. He is a professor at Osaka University, Japan. His current research interests include ultimate strength of ships and offshore structures, risk assessment of ships and offshore structures, nonlinear structural analysis of large plated structures, and the Idealized Structural Unit Method (ISUM).